Solar-Terrestrial Physics, 2016. Vol. 2. Iss. 4, pp. 55–69, DOI: 10.12737/24273. © INFRA-M Academic Publishing House
Original Russian version A.G. Kim, S.N. Ponomarchuk, G.V. Kotovich, E.B. Romanova,
published in Solnechno-Zemnaya Fizika, 2016, vol. 2, iss. 4, pp. 43–53, DOI 10.12737/21815

MODELING Z-SHAPED DISTURBANCE ALONG THE PEDERSEN RAY OF OBLIQUE SOUNDING IONOGRAM USING ADAPTATION OF IRI TO EXPERIMENTAL DATA

A.G. Kim, S.N. Ponomarchuk, G.V. Kotovich, E.B. Romanova

Institute of Solar-Terrestrial Physics SB RAS, Irkutsk, Russia, kim_anton@mail.ru
spon@iszf.irk.ru, kotovich@iszf.irk.ru, ebr@iszf.irk.ru

We present the results of numerical modeling of a traveling ionospheric disturbance that causes z-shaped bends at the Pedersen ray of oblique incidence ionograms. The results of trajectory synthesis of oblique incidence ionograms are given for the ionosphere, taking into account the traveling ionospheric disturbance. In the work, we use the International Reference Ionosphere, adapted to experimental data, and the Global Model of the Ionosphere and Plasmasphere.

Keywords Ionosphere · Oblique sounding · Ionogram · Traveling ionospheric disturbance

---

INTRODUCTION

Ionospheric irregularities, including traveling ionospheric disturbances (TIDs), have been studied in many papers [Maeda, Handa, 1980; Ivanov et al., 1987; Boytman, Kalikhman, 1989; Vugmeyster et al., 1993; Millward et al., 1993; Hocke, Schlegel, 1996; Afraimovich et al., 2002; Ding et al., 2008]. Along with diurnal and seasonal variations of ionospheric parameters (large-scale irregularities) at ionospheric heights there are traveling ionized structures of small and medium scales.

Despite the emergence and development of space-based sensing instruments, which gave an opportunity to obtain data on the Total Electron Content [Afraimovich, Perevalova, 2006], ionospheric research with the aid of frequency-modulated continuous wave ionosondes is relevant and sometimes the only way to gain information about a communication channel. It is important to understand factors that cause distortions of distance-frequency characteristic (DFC) of oblique sounding (OS) and to deviations from mean diurnal variations in maximum observed frequencies (MOF). MOF variations with periods of more than one hour on OS paths can be attributed to large-scale TIDs passing the sounding path at F-region heights [Kutelev, Kurkin, 2011]. MOF variations with shorter periods often occur with z-shaped bends in the single-hop 1F2-mode in DFC [Vertogradov et al., 2008], which move in the course of time along the upper ray (Pedersen) from the region of higher delays to the region of lower ones (sometimes repeating this movement several times).

The purpose of this study is to model TID that causes z-shaped bends at the Pedersen ray in DFC. To simulate the propagation medium, we employ the following models: International Reference Ionosphere (IRI) with correction over real observations and the Global Model of the Ionosphere and Plasmasphere (GMIP) developed in ISTP SB RAS.

MODELING DFC

DFC of a signal is calculated using the geometrical optics approximation [Kravtsov and Orlov, 1980]. The software is implemented with the method of characteristics [Golygin et al., 2003; Mikhailov, Kurkin, 2007]. Under this approach, a path problem is solved based on numerical integration of a system of characteristic equations for a two-dimensional case, using the Runge-Kutta method of the forth order of accuracy [Bakhvalov et al., 2001]:

$$\frac{dr}{d\tau} = p_r,$$

$$\frac{d\varphi}{d\tau} = \frac{1}{r} p_\varphi,$$

$$\frac{dp_r}{d\tau} = -\frac{f_{pe}}{f^2}\frac{\partial f_{pe}}{\partial r} + \frac{1}{r} p_\varphi^2,$$

$$\frac{dp_\varphi}{d\tau} = -\frac{1}{r}\left(\frac{f_{pe}}{f^2}\frac{\partial f_{pe}}{\partial \varphi} + p_r p_\varphi \right),$$

where r, φ are polar coordinates in the plane of the radio path with respect to Earth's center, τ is the group path (propagation time multiplied by the speed of light), f_{pe} is the plasma frequency, f is the signal frequency, p_r, p_φ are components of the orienting pulse $\vec{p}$ (equal to the absolute value of refractive index n at a tangent to the trajectory in the direction of propagation). To compensate for a computational error, we make a step-by-step test to meet the eikonal equation $p_r^2 + p_\varphi^2 = n^2$ and, if necessary, correct the orienting pulse in magnitude $\vec{p}$.

The propagation medium is specified, taking into account results obtained in [Kiyanovsky, Sazhin, 1980], by evenly spaced vertical profiles of plasma frequency (with a step of 10 km) along the path in the great-circle arc (with a distance of ~ 80 km between nodal points). Characteristics of the propagation medium are approximated through application of second-degree two-dimensional local B-splines on a uniform grid of values [Konoplin, Orlov, 1981] for the plasma frequency and for its partial derivatives. Input parameters for calculations are taken such that the calculating time is optimal. In most cases, the integration step is 1 km. The calculation in nodes of reference values of partial derivatives is based on plasma frequency interpolation by a Lagrange polynomial:

$$f'(k) = \sum_{i=1}^{k-1} \frac{(k-1)!(N-k)!(-1)^{k-i}}{(k-i)(i-1)!(N-i)!} f(i) + f(k) \times \sum_{\substack{i=1 \\ i \neq k}}^{N} \frac{1}{k-i} + \sum_{i=k+1}^{N} \frac{(k-1)!(N-k)!(-1)^{i-k-1}}{(i-k)(i-1)!(N-i)!} f(i),$$

where $k = 1, ..., N$.

MODELING TID BY IRI

Ionograms often have various DFC distortions manifesting themselves as bends, loops, scattering, etc. Figure 1 shows OS ionograms with traces of TIDs obtained on two paths (Figure 2) over the observation period from March 29 to April 2, 2004.

Transmitters are located in Magadan (60° N, 150.7° E) and Khabarovsk (48.5° N, 135.1° E). A receiver is in the Tunka valley in the village of Tory (51.8° N, 103° E), at about one hundred kilometers from Irkutsk (52° N, 104° E). The length of the Khabarovsk–Tory path is ~ 2300 km; Magadan–Tory path is ~ 3030 km. The distance between the midpoints of the Khabarovsk–Tory (51.26° N, 119.57° E) and Magadan–Tory (58.2 ° N, 124.17 ° E) paths is ~ 825 km.

We can see (Figure 1) that these DFC have traces of reflections that are not characteristic of the spherically stratified ionosphere or the ionosphere with a weak horizontal gradient. The geomagnetic activity index K_p in this period did not, on average, exceed 3. However, despite Earth's magnetic field was relatively quiet those days, at certain moments there were fairly stable z-shaped or sickle-shaped bends ("sickles") in the single-hop 1F2-mode of DFC, which moved in the course of time from the region of higher delays to the region of lower ones.

Numerical modeling with geometrical optics approximation is widely used to study TID effects on characteristics of decameter radio waves. For example, in [Balagansky, Sazhin, 2003], disturbances on OS ionograms are interpreted through numerical modeling of three-dimensional inhomogeneous wave-like TIDs for the global ionospheric model with correction. An attempt to interpret OS ionograms with z-shaped distortions at the Pedersen ray (Figure 1) was made in [Kopka, Möller, 1968], in which the authors carried out computer simulation to study effects of small horizontal variations in a layer height for a single-layer parabolic ionospheric model on 2000 and 8000 km paths. Unlike [Kopka, Möller, 1968], in this work we run simulation for conditions of the real path (Khabarovsk–Tory, the range is ~ 2300 km) over the full ionospheric profile with gradient, adapting the IRI model [Kotovich, Mikhailov, 2003].

The joint application of ionospheric models, adaptation techniques, methods for calculating propagation characteristics, and experimental data, acquired on OS paths, improves the accuracy of interpretation of observations. To adapt the IRI model, we use VS data obtained near transmission and reception points; and to acquire data at the midpoint of the path, we utilize a method of converting experimental DFC into height-frequency characteristic (VFC) [Kim et al., 2004]. The OS data conversion algorithm provides VFC for the midpoint of the path, but the ionospheric model can be corrected using only f_0F2.

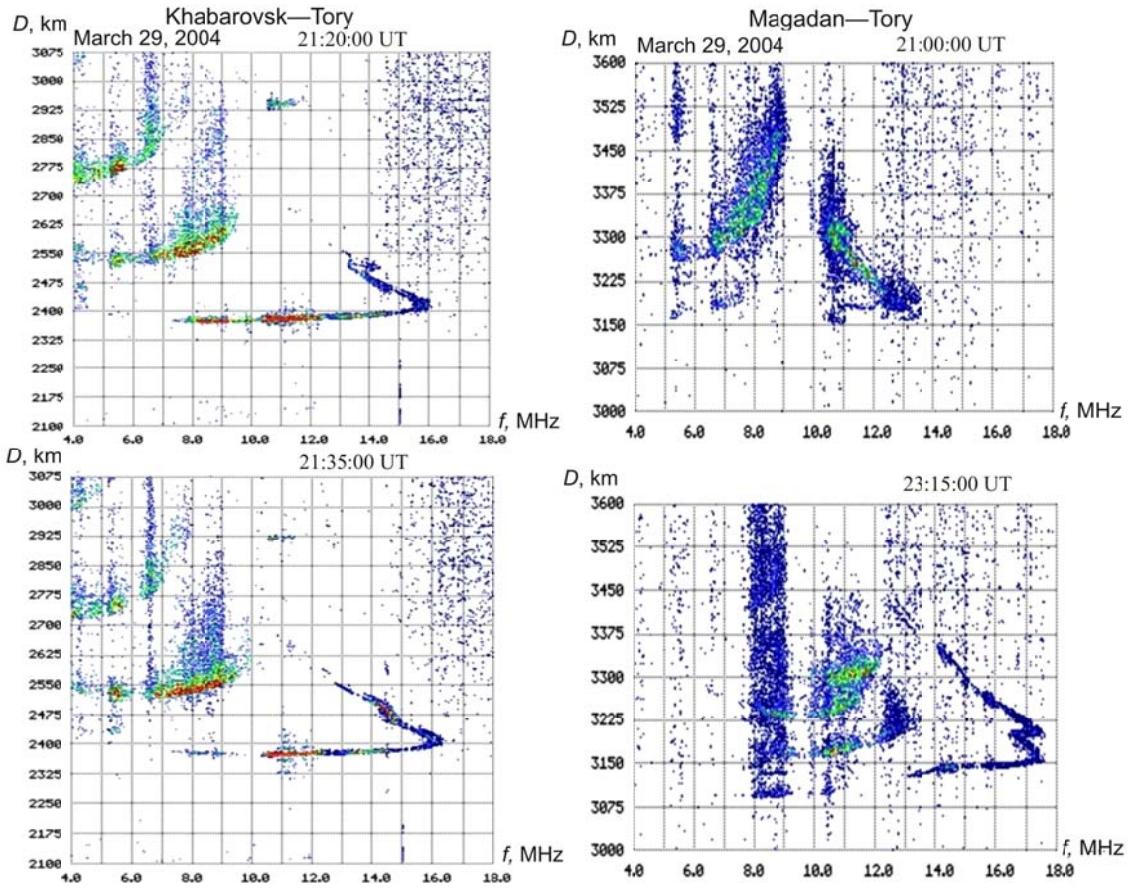

Figure 1. TIDs on OS ionograms obtained over Khabarovsk–Tory and Magadan–Tory paths

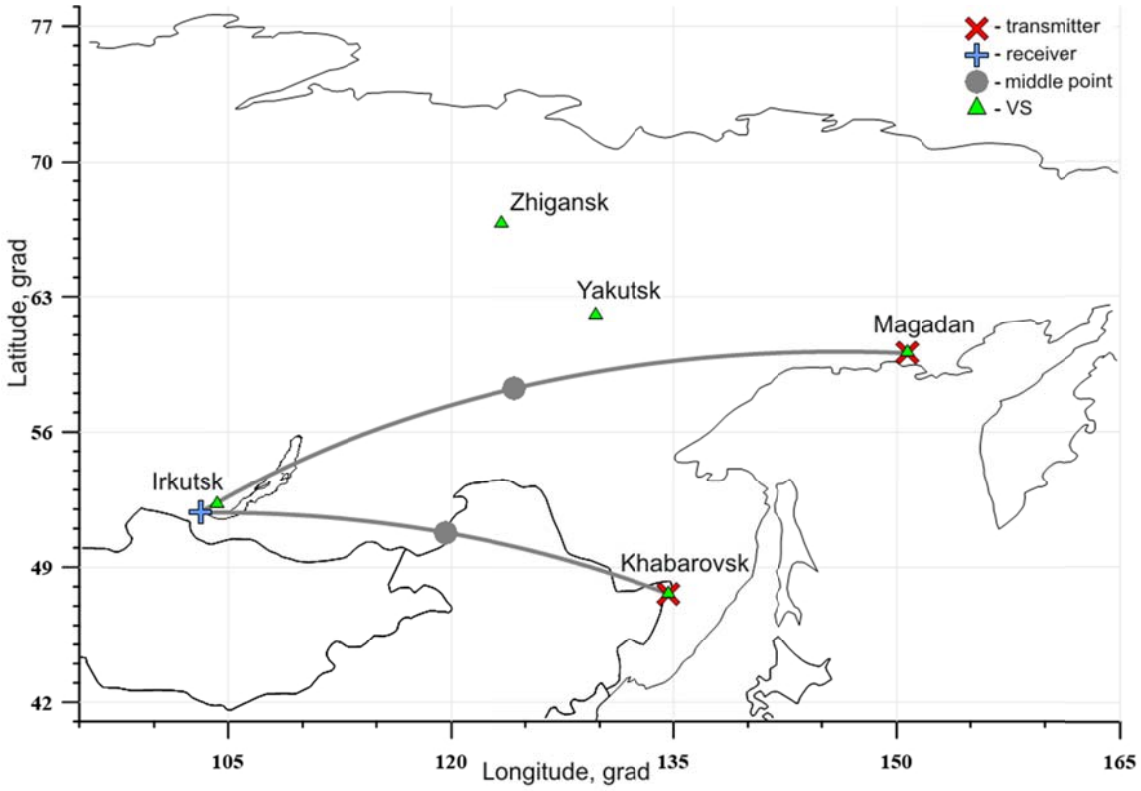

Figure 2. Map of paths

Therefore, processing of OS ionograms provides a set of MOF; and for the highest point at the upper ordinary ray of the 1F2-mode (whose path before reflection is close to the Pedersen ray passing the maximum ionization height in the vicinity of the midpoint of the path), frequency and absolute time of signal propagation are also stored. These data and the modified Smith method [Kiyanovsky, 1971] are used to compute f_oF2 at the midpoint of the path by the algorithm described in [Kotovich et al., 2006]. Then, values of the vertical electron density profile obtained with the IRI model are adapted from f_oF2 values acquired at endpoints and calculated for the midpoint of the path.

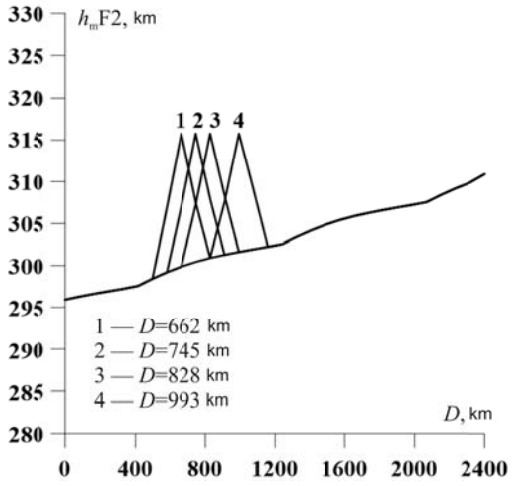

Figure 3. Disturbance model for h_mF2

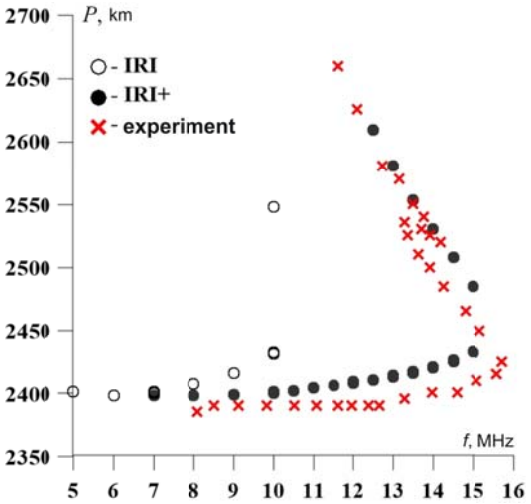

Figure 4. Estimated DFC without disturbance

Yet f_0F2 values between three points along the path are linearly interpolated.

The propagation medium is interpolated along the path between 29 nodal points given by evenly spaced vertical plasma frequency profiles along the great-circle arc.

Since the upper ray is formed at heights near the F2-layer maximum [Davies, 1965], we assume that the distortion at the upper ray are caused by TIDs located at a close height level. According to the OS data, h_mF2 ranged from 290 to 300 km in Khabarovsk, and from 300 to 320 km in Irkutsk; therefore in

modeling we specify a linear variation in h_mF2 along the path (from a transmitter to a receiver) from 295 to 310 km. The increase in height of the simulated disturbance of the F2-layer peak electron density at 15 km from the middle of the background curve corresponds to 315 km (Figure 3). In this case, we simulate a triangular-shaped disturbance with a base width of ~ 328 km.

In Figure 4, unshaded circles indicate the estimated DFC for March 29, 21:00 UT (medium parameters are given by the IRI model, adapted from the average monthly index $F10.7 = 111$). Shaded circles show the calculated DFC after the adaptation of the IRI model from three parameters: $F10.7$ (we use the same monthly average), critical frequencies at three points of the path (via linear interpolation along the path), and maximum heights at two (end) points of the path. The experimental DFC is marked with crosses. After the IRI model adaptation has been completed, the deviation of the obtained maximum usable frequency (MUF) from MOF observed in the experiment is only 2 %.

Figure 5 illustrates the simulated abnormal DFC with horizontal movement of the h_mF2 disturbance (Figure 3) along the path (from a transmitter to a receiver) at 662, 745, 828, and 993 km from the transmitter.

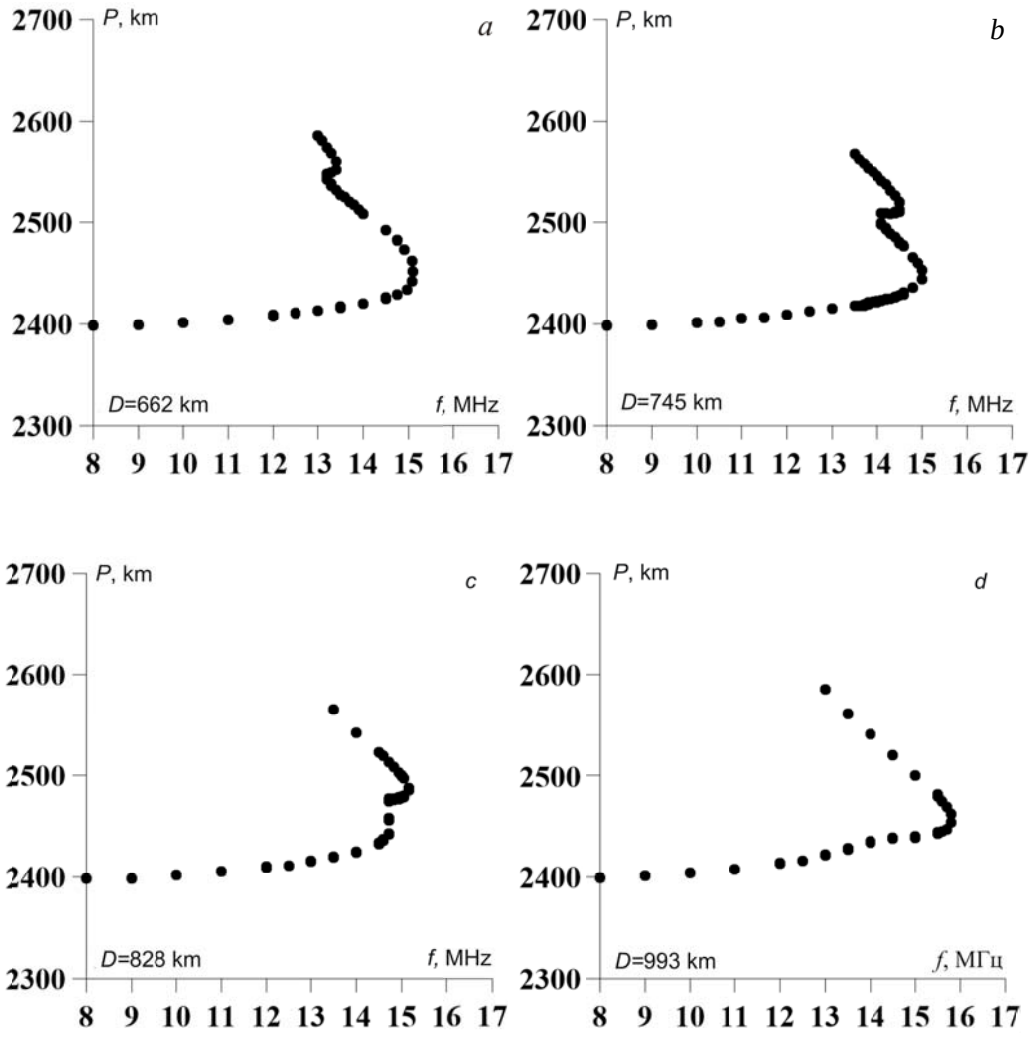

Figure 5. Estimated DFC during the h_mF2 disturbance

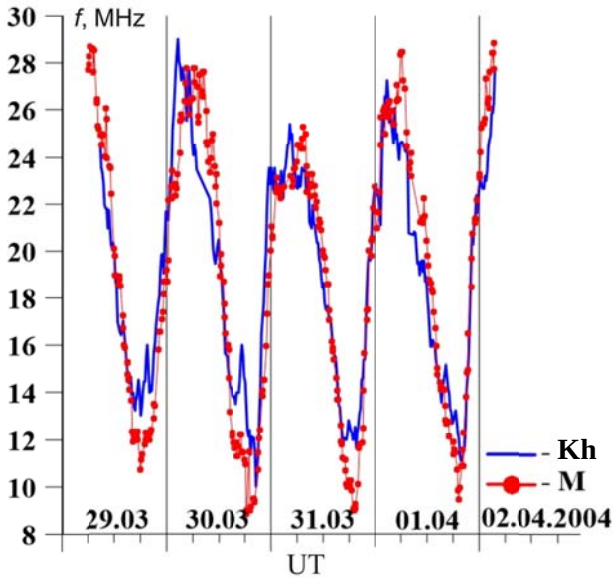

Figure 6. The diurnal variation of MOF for Khabarovsk–Tory (Kh) and Magadan–Tory (M) paths

As the disturbance approaches the midpoint of the path, MUF increases (Figure 5, *d*). When such a disturbance propagates over a larger distance, there are no significant changes along the upper ray in the estimated DFC.

The correlated variability of the diurnal MOF variation on two adjacent paths (Figure 2) can show the presence of a moving irregularity at h_mF2. From March 30 to April 1, 2004, maxima in the diurnal variation of MOF of the paths under study were shifted in time (Figure 6). Knowing the distance between midpoints of the paths (~ 825 km) and their coordinates, we qualitatively estimated the velocity and direction of irregularity. Apparently, the disturbance was positive; and the MOF increase observed first on the Khabarovsk–Tory path and then on the Magadan–Tory one testifies that the irregularity moved from south to north. The time delay between the disturbance manifestations suggests that its velocity was ~ 70–100 m/s.

The analysis of MOF aimed at determining TID parameters is described in more detail in [Ivanov et al., 2006]. In addition, the lifetime and sizes of TIDs can be judged by the dynamics of "sickle" movement along the upper ray. As deduced from the experimental OS data, the duration of such distortions ranged from 15 min to several hours. Given typical TID velocities of ~ 100 m/s, this corresponds to horizontal TID dimensions of ~ 90 km registered over ~ 1000 km. The minimum distance of 90 km depends on the detection interval. In fact, such irregularity can be less than 90 km because deformation of the upper ray during a session can be detected only in single DFC (rather than in several ones in a row).

MODELING TID BY GMIP

Unlike the semi-empirical IRI model, the ISTP-developed global model of the ionosphere and plasmasphere enables us to use a minimum set of input data to calculate vertical profiles of electron density and effective collision frequency, taking into account physical processes in Earth's upper atmosphere

[Krinberg, Tashchilin, 1984; Tashchilin, Romanova, 2002; Tashchilin, Romanova, 2013]. This model is used to calculate ionospheric parameters in extreme conditions, i.e. during magnetic storms and solar flares. An important role is played here by electron density variations in the lower region of the ionosphere (E layer) during these periods as compared to the background undisturbed ionosphere because they can substantially increase signal absorption. GMIP, as other ionospheric models, retains seasonal diurnal variations in ionospheric parameters, their dependence on solar activity, season, time of day, as well as on coordinates (latitude, longitude) of radio path's point of signal propagation, and takes into account the horizontal ionospheric irregularity at dawn and dusk hours. The complex algorithm including blocks for calculating GMIP and conditions of HF radio wave propagation allows us to compute distance-frequency and angular frequency characteristics of signals [Ponomarchuk et al., 2015].

The software package for calculating DFC enables us to represent all major propagation modes of a signal reflected from the regular ionospheric layers (E, F1, F2). Figure 7, *a* shows a typical DFC obtained on the Khabarovsk–Irkutsk path on March 7, 2015 at 00:36 UT. Lines depict DFC of the propagation modes 1F2, 2F2, and 3F2 calculated in the geometrical optics approximation.

Figure 7, *b*, *c*, *d* presents OS ionograms with traces of disturbances obtained on the Khabarovsk–Irkutsk path on March 7, 2015 at 00:56 UT, 01:06 UT, and 02:06 UT respectively. Approximately one hour after the disturbance commencement, on the ionograms there were no bends at the upper ray; and TID effects caused MOF to increase.

Internal gravity waves (IGW), which always exist in the thermosphere, play an important role in the formation of electron density irregularities in the F-region. Ionospheric effects of propagating IGW is TID, i.e. rise and subsequent fall of the F2 layer as IGW passes over the station, which usually occurs with a phase-shifted change in the electron density at the F2-layer maximum. Since the main mechanism of IGW influence on F-layer plasma is the transfer of momentum of horizontally moving neutral particles to ions, which thus acquire an additional velocity along the magnetic field, when simulating TID we specify wind momentum at a given point of the path.

To preset the propagation medium at each point of the path, we calculate the vertical profile of ionospheric parameters, using GMIP. GMIP has been developed from two models: the global semi-empirical prediction model for the D-region designed to calculate ionization in the lower ionosphere (40–100 km), and the Theoretical Model of the Ionosphere and Plasmasphere for calculating ionization at a height above 100 km.

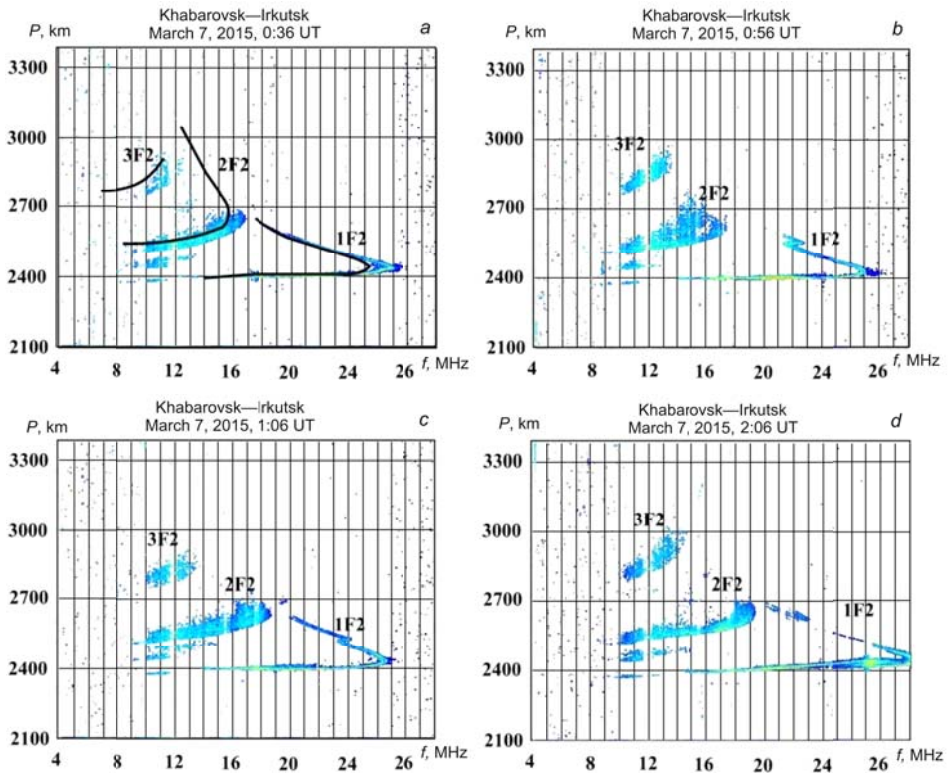

Figure 7. OS ionograms obtained over the Khabarovsk–Irkutsk path on March 7, 2015: 00:36 UT (*a*), 00:56 UT (*b*), 01:06 UT (*c*), 02:06 UT (*d*)

The Theoretical Model of the Ionosphere and Plasmasphere accounts for the plasma drift across geomagnetic field lines [Krinberg, Tashchilin, 1984; Tashchilin, Romanova, 1995, 2002; Tashchilin, Romanova, 2013]. In the model, the molecular ions N_2^+, NO^+, and O_2^+ are considered as the ion M^+ of mass 30 amu with the ion density described as $N(M^+)=n(N_2^+)+n(NO^+)+n(O_2^+)$. The model provides densities of ions of hydrogen $N(H^+)$, helium $N(He^+)$, oxygen $N(O^+)$, molecular ions $N(M^+)$, and electrons $N_e = N(H^+)+N(He^+)+N(O^+)+N(M^+)$, electron T_e and ion T_i temperatures along the geomagnetic field at $h \geq 100$ km from this ionospheric region to the magnetoconjugated one.

This model is based on the numerical solution of unsteady-state equations for particle balance and thermal plasma energy in drifting plasma tubes of dipole type, bases of which are at a height of 100 km. Densities of all ions are calculated taking into account photoionization, recombination, and transfer along geomagnetic field lines under the action of ambipolar diffusion and ion entrainment with the horizontal neutral wind. To calculate rates of photoionization of thermospheric components and energy spectra of primary photoelectrons, we use the reference spectrum of solar UV radiation from [Richards et al., 1994]. Electron and ion temperatures are computed making allowance for the thermal conductivity along geomagnetic field lines and the heat exchange between electrons, ions, and neutral particles due to elastic and inelastic collisions. The heating rate of thermal electrons is calculated consistently by solving the kinetic equation for photoelectron transfer in conjugate ionospheric regions with respect to energy losses by photoelectrons in passing through the plasmasphere.

To describe spatio-temporal variations in temperature and neutral densities of O, O_2, N_2, H, and N, we employ the global empirical model of the thermosphere NRLMSISE-00 [Picone et al., 2002] and determine velocities of the horizontal thermospheric wind by the empirical models HWM07 [Drob et al., 2008] and DWM07 [Emmert et al., 2008]. The values of the integral flux and mean energy of precipitating electrons necessary to calculate auroral ionization rates are taken in accordance with the global model of electron precipitation [Hardy et al., 1987]. The electric field of magnetospheric convection is calculated with the empirical model of distribution of magnetospheric convection potential at ionospheric heights [Sojka et al., 1986].

TIDs can be driven by large-scale IGWs propagating equatorward of the auroral heating source [Afraimovich et al., 2002]. Such a wave can be a momentum of the equatorward wind with its velocity depending on height. In the presence of the thermospheric wind, ions and electrons are subject to a friction force. Since charged particles are free to move only along the geomagnetic field [Rishbeth, Garriott, 1969], the longitudinal friction force component (in the case of the equatorward wind) will transfer charged particles up along the inclined geomagnetic field lines (Figure 8). This movement will cause the F2 layer to rise. The longitudinal component $U_{||}$ and the vertical component of the W_{wind} drift driven by the thermospheric wind are calculated as follows:

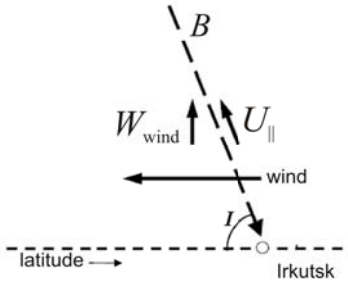

Figure 8. Thermospheric wind effect on a charged component

$$U_{||} = (U\cos D - V\sin D)\cos I,$$

$$W_{\text{wind}} = U_{||}\sin I,$$

where U and V are meridional and zonal components of the horizontal thermospheric wind, I and D are magnetic inclination and declination (for Irkutsk, $I = 72.2°$, $D = -3.86°$).

TID passage over a given point of the path is modeled as strengthening of W_{wind}:

$$W_{\text{wind}} + 50\ [\text{m/s}] \cdot \text{WTID},$$

where WTID is a coefficient, which enables us to change the momentum. In the model calculations, we use WTID = 0.5, i.e. W_{wind} increased by 25 m/s. Such a momentum is specified at nodal points along the propagation path successively from a transmitter to a receiver.

This disturbance from GMIP is modeled for the Khabarovsk–Irkutsk path (March 7, 2015, 01:00 UT) with subsequent calculation of DFC in the geometrical optics approximation. In the modeling, we assume that an irregularity should cover a space near the path such that reflection points are in the plane

of the great-circle arc and signal paths fall into a receiving point. The paths that deviate from the great-circle arc are not considered.

Figure 9 shows levels of plasma frequencies as a function of height and propagation path of a 23.2 MHz signal with respect to medium disturbances. The irregularity is situated at ~ 634 km from the transmitter. The propagation medium is specified by evenly spaced vertical electron density profiles at 30 points along the great-circle arc. The step of calculation between adjacent nodal points is ~ 79 km. The modeling reveals that in the vicinity of the turning point nearby the disturbance, upper rays are focused.

Figure 10 illustrates paths for the 24 MHz signal for the same instant. At the given frequency, upper rays do not diverge. Thus, the irregularity has an effect on the group path of the upper ray only when the wave disturbance is maximal along the great-circle arc from the point of signal entry into the ionosphere to the midpoint of the path (Figure 11).

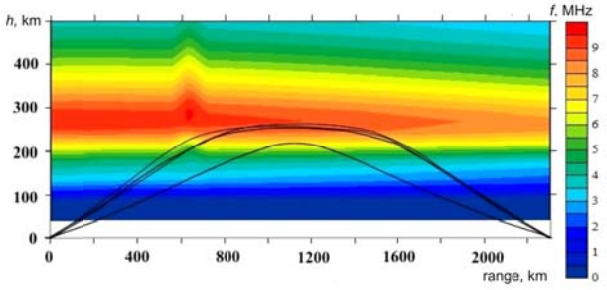

Figure 9. Paths of signal propagation in the disturbed ionosphere: f = 23.2 MHz

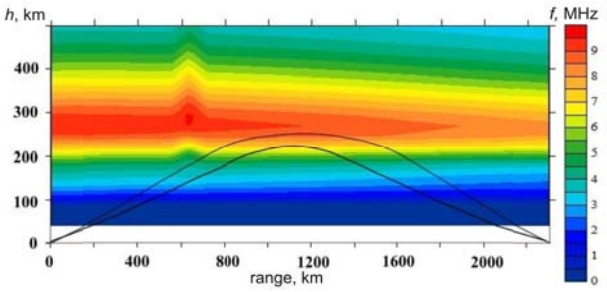

Figure 10. Paths of signal propagation in the disturbed ionosphere: f = 24 MHz

If the maximum of irregularity shifts to the midpoint of the path, MUF increases (Figure 11, *d*). If the disturbance is in the second half of the path out of the reflection point, there is no TID effect at the upper ray in DFC (Figure 11, *e*). This is also confirmed by [Kopka, Möller, 1968; Grozov et al., 2005].

Thus, the qualitative modeling has shown that the time displacement of such sickle-shaped bends along the upper ray of the single-hop 1F2- mode in DFC (Figure 11) can be caused by a gust of the thermospheric wind with a speed of +25 m/s relative to the background one.

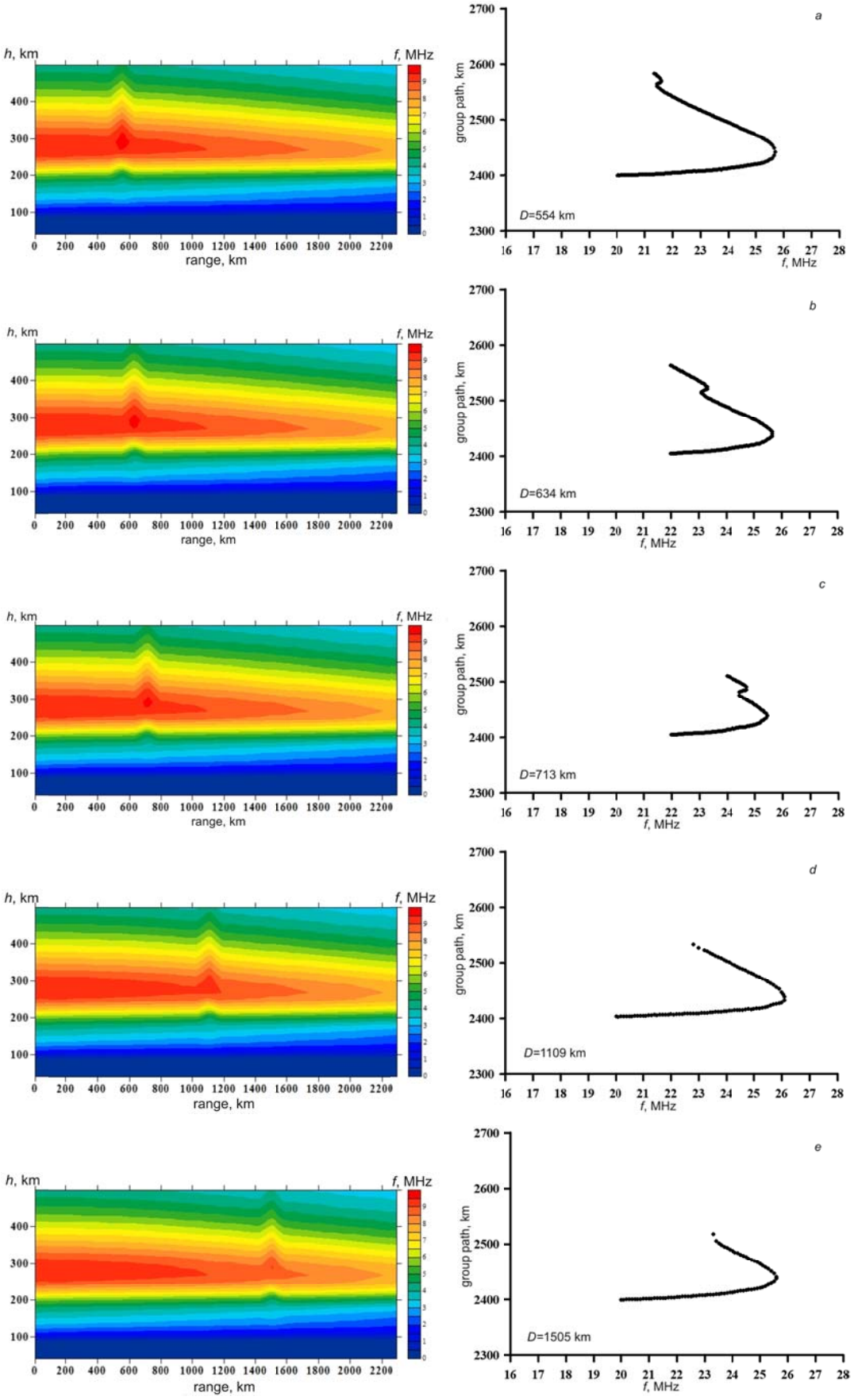

Figure 11. Simulation results for disturbance (left) and DFC (right)

CONCLUSION

Using the ionospheric model adapted from experimental data, we have tested the disturbance model accounting for the change in h_mF2in local sections of the OS path. We have shown that OS ionograms with z-shaped bends in the vicinity of the upper ray, which are not characteristic of the spherically stratified ionosphere or the ionosphere with a weak horizontal gradient, may indicate that at the moment of formation of a reflected signal, it is reflected and focused from the region of the h_mF2 local jump occurring in the first half of the path. The modeling has also revealed that with TID passing nearby the midpoint of the OS path, bends at the upper ray disappear and MOF increases. This can be used to obtain TID parameters by analyzing MOF variations from observations acquired at the network of OS paths. If the jump of h_mF2 falls on the second half of the path, there is no z-shaped bend at the upper ray of the single-hop mode 1F2.

The ISTP-developed global model of the ionosphere and plasmasphere allowed us to attribute the local change in h_mF2 to the influence of the thermospheric wind differing from the background wind by 25 m/s.

The method of correcting the IRI model from experimental OS data can also be used to correct other ionospheric models capable of adapting from f_0F2. The necessary conditions are the availability of reliable experimental OS data and the possibility of obtaining parameters of the single-hop 1F2-mode. The process of adaptation of the ionospheric model can be employed to solve the inverse problem in interpreting experimental data.

We are grateful to A.V. Tashchilin and A.V. Oinats for useful consultations.

REFERENCES

Afraimovich E.L., Perevalova N.P. *GPS-monitoring verkhnei atmosfery Zemli* [GPS-Monitoring of the Earth's Upper Atmosphere]. Irkutsk, 2006, 480 p. (In Russian).

Afraimovich E.L., Ashkaliev Ya.E., Aushev V.M. Beletsky A.B., Vodyannikov V.V., Leonovich L.A., Lesyuta O.S., Mikhalev A.V., Yakovets A.F. Simultaneous radio and optical observations of the mid-latitude atmospheric response to a major geomagnetic storm of 6–8 April 2000. *J. Atmos. and Sol.-Terr. Phys* . 2002, vol. 64, no. 18, pp. 1943–1955.

Afraimovich E.L., Voeykov S.V., Perevalova N.P. Traveling wave disturbance of total electron content according to worldwide GPS network (morphology and dynamics). *Solnechno-zemnaya fizika* [Solar-Terrestrial Physics]. 2002, iss. 3, pp. 61–72. (In Russian).

Balaganskiy B.A., Sazhin V.I. Numerical modeling of HF radio wave characteristics in the ionosphere with third-dimensional inhomogeneous disturbances // *Geomagnetizm i aeronomiya* [Geomagnetism and Aeronomy], 2003, vol. 43, no. 1, pp. 92–96. (In Russian).

Bakhvalov N.S., Zhidkov N.P., Kobelkov G.M. *Chislennye metody* [Numerical Methods]. FML Publ., 2001. 630 p. (In Russian).

Boitman O.N., Kalikhman A.D. Analysis of traveling ionospheric disturbances structure with the help of ionograms. *Issledovaniya po geomagnetizmu, aeronomii i fizike Solntsa* [Geomagnetism, Aeronomy and Solar Physics

Research], Moscow, Nauka Publ., 1989, vol. 88, pp. 59–69. (In Russian).

Davies K. *Ionospheric Radio Propagation*. U.S. Department of Commerce, National Bureau of Standards, 1965. 470 p.

Ding F., Wan W., Liu L., Afraimovich E.L., Voeykov S.V., Perevalova N.P. Statistical study of large scale traveling ionospheric disturbances observed by GPS TEC during major magnetic storms over the years 2003-2005. *J. Geophys. Res*. 2008, vol. 113, A00A01.

Drob D.P., Emmert J.T., Crowley G., Picone J.M., Shepherd G.G., Skinner W., Hays P., Niciejewski R.J., Larsen M., She C.Y., Meriwether J.W., Hernandez G., Jarvis M.J., Sipler D.P., Tepley C.A., O'Brien M.S., Bowman J.R., Wu Q., Murayama Y., Kawamura S., Reid I.M., Vincent R.A. An empirical model of the Earth's horizontal wind fields: HWM07. *J. Geophys. Res.* 2008, vol. 113, A12304. DOI: 10.1029/2008 JA013668.

Emmert J.T., Drob D.P., Shepherd G.G., Hernandez G., Jarvis M.J., Meriwether J.W., Niciejewski R.J., Sipler D.P., Tepley C.A. DWM07 global empirical model of upper thermospheric storm-induced disturbance winds. *J. Geophys. Res*. 2008, vol. 113, A11319. DOI: 10.1029/2008JA013541.

Golygin V.A., Mikhailov Ya.S., Sazhin V.I. Numerical modeling of oblique ionograms with propagation in ionospheric channels. *Baikal'skaya mezhdunarodnaya molodezhnaya shkola po fundamentalnoi fizike: trudy* [Proc. Baikal Young Scientists` International School on Fundamental Physics], Irkutsk, 2003, pp. 75–77. (In Russian).

Grozov V.P., Dumbrava Z.F., Kim A.G., Kotovich G.V., Mikhailov Ya.S., Oinats A.V. Traveling ionospheric disturbances from oblique ionograms and modeling of disturbance parameters. *Rasprostranenie radiovoln: sbornik dokladov XXI Vserossiyskoi nauchnoi konferentsii* [Radio Propagation: Proc. XXI Russian National Conf.], Yoshkar-Ola, 25–27 May 2005, vol. 1, pp. 177–181. (In Russian).

Hardy D.A., Gussenhoven M.S., Raistrick R., McNeil W.J. Statistical and functional representation of the pattern of auroral energy flux, number flux, and conductivity. *J. Geophys. Res*. 1987, vol. 92, pp. 12275–12294.

Hocke K., Schlegel K. A review of atmospheric gravity waves and travelling ionospheric disturbances: 1982–1995. *Ann. Geophys*. 1996, vol. 14, pp. 917–940.

Ivanov V.P., Karvetskiy V.L., Koren`kova N.A. Seasonal-diurnal variations of middle scale traveling ionospheric disturbances. *Geomagnetizm i aeronomiya* [Geomagnetism and Aeronomy]. 1987, vol. 27, no. 3, pp. 511–513. (In Russian).

Ivanov V.A., Lyong V.L., Nasyrov A.M., Ryabova N.V. Modeling of ionograms for traveling ionospheric disturbances research and its connection with maximal observing frequencies. *Georesursy* [Georesources]. 2006, no. 2 (19), pp. 2–5. (In Russian).

Kim A.G., Grozov V.P., Kotovich G.V. Application of modified method of transferring curves for critical frequency calculation from Pedersen ray in path midpoint. *Mezhdunarodnaya Baikal'skaya molodezhnaya shkola po fundamentalnoi fizike: trudy* [Proc. Baikal Young Scientists` International School on Fundamental Physics]. Irkutsk, 2004, pp. 82–85. (In Russian).

Kiyanovsky M.P. Computer calculations with the help of the modified method of transfer curves. *Luchevoe priblizhenie i voprosy rasprostraneniya radiovoln* [Geometric optics and radio propagation]. Moscow, Nauka Publ., 1971, pp. 287–298. (In Russian).

Kiyanovsky M.P., Sazhin V.I. On the analytical representation of ionospheric data in calculating decameter radio wave propagation. *Issledovaniya po geomagnetizmu, aeronomii i fizike Solntsa* [Geomagnetism, Aeronomy and Solar Physics Research]. Moscow, Nauka Publ., 1980, iss. 51, pp. 41–48. (In Russian).

Konoplin V.N., Orlov A.I. Data approaching by local second-order splines. *Issledovaniya po geomagnetizmu, aeronomii i fizike Solntsa* [Geomagnetism, Aeronomy and Solar Physics Research]. Moscow, Nauka Publ., 1981, iss. 57, pp. 101–104. (In Russian).

Kopka H., Möller H.G. Interpretation of anomalous oblique incidence sweep-frequency records using ray tracing. *Radio Sci*. 1968, vol. 3, no. 1, pp. 43–51.

Kotovich G.V., Mikhailov S.Ya. Adaptive Abilities of IRI model in predicting decametric radiopath characteris-

tics. *Geomagnetism and Aeronomy*. 2003, vol. 43, no. 1, pp. 82–85.

Kotovich G.V., Kim A.G., Mikhailov S.Ya., Grozov V.P., Mikhailov Ya.S. Determining the f_oF2 critical frequency at the path midpoint from oblique sounding data based on the Smith method. *Geomagnetism and Aeronomy*. 2006, vol. 46, no. 4, pp. 517–521.

Kravtsov Yu.A., Orlov Yu.I. *Geometricheskaya optika neodnorodnykh sred* [Geometric optics for non-homogeneous media]. Moscow, Nauka Publ., 1980. 304 p. (In Russian).

Krinberg I.A., Tashchilin A.V. *Ionosfera i plazmosfera* [Ionosphere and Plasmasphere]. Moscow, Nauka Publ., 1984, 189 p. (In Russian).

Kutelev K.A., Kurkin V.I. Modeling impact of large-scale wavelike traveling ionospheric disturbances on oblique ionograms for Irkutsk–Norilsk and Irkutsk–Magadan paths. *Rasprostranenie radiovoln: sbornik dokladov XXIII Vserossiiskoi nauchnoi konferentsii* [Radio Propagation: Proc. XXIII Russian National Conf.], Yoshkar-Ola, 23–26 May, 2011, vol. 1, pp. 235–238. (In Russian).

Maeda S., Handa S. Transmission of large-scale TIDs in the ionospheric F2-region. *J. Atmos. Terr. Phys*. 1980, vol. 42, no. 9/10, pp. 853–859.

Mikhailov Ya.S., Kurkin V.I. Research of parameters of traveling ionospheric disturbances. *Mezhdunarodnaya Baikal'skaya molodezhnaya shkola po fundamentalnoi fizike: trudy* [Proc. Baikal Young Scientists` International School on Fundamental Physics]. Irkutsk, 2007, pp. 164–167. (In Russian).

Millward G.H., Moffett R.J., Quegan S., Fuller-Rowell T.J. Effects of an gravity wave on the midlatitude ionospheric F layer. *J. Geophys. Res*. 1993, vol. 98, pp. 19173–19179.

Picone J.M., Hedin A.E., Drob D.P., Aikin A.C. NRLMSISE-00 empirical model of the atmosphere: Statistical comparisons and scientific issues. *J. Geophys. Res*. 2002, vol. 107, no. A12, pp. 1468–1483.

Ponomarchuk S.N., Kotovich G.V., Romanova E.B., Tashchilin A.V. Forecast of short radio waves characteristics on the base of Global ionosphere and plasmasphere model. *Solnechno-zemnaya fizika* [Solar-Terrestrial Physics]. 2015, vol. 1, no. 3, pp. 49–54. (In Russian).

Richards P.G., Fennelly J.A., Torr D.G. EUVAC: solar EUV flux model for aeronomic calculations. *J. Geophys. Res*. 1994, vol. 99, no. A5, pp. 8981–8992.

Rishbeth H., Garriott O.K. *Introduction to Ionospheric Physics*. New York, Academic Press, 1969. 334 p.

Sojka J.J., Rasmussen C.E., Schunk R.W. An interplanetary magnetic field dependent model of the ionospheric convection electric field. *J. Geophys. Res*. 1986, vol. 91, pp. 11281–

Tashchilin A.V., Romanova E.B. UT-control effects in the latitudinal structure of the ion composition of the topside ionosphere. *J. Atmos. and Terr. Phys*. 1995, vol. 57, no. 12, pp. 1497–1502.

Tashchilin A.V., Romanova E.B. Numerical modeling the high-latitude ionosphere. *Proc. COSPAR. Colloquia Series*. 2002, vol. 14, pp. 315–325.

Tashchilin A.V., Romanova E.B. Numerical modeling of ionosphere scattering in dipole geomagnetic field with crossover drift. *Matematicheskoe modelirovanie* [Mathematical modeling]. 2013, vol. 25, no. 1, pp. 3–17. (In Russian).

Vertogradov G.G., Denisenko P.F., Vertogradova E.G., Uryadov V.P. The monitoring of medium-scale travelling ionospheric disturbances as the result of oblique chirp sounding of the ionosphere. *Elektromagnitnye volny i elektronnye sistemy* [Electromagnetic Waves and Electronic Systems]. 2008, vol. 13, no. 5, pp. 35–44. (In Russian).

Vugmeister B.O., Zakharov V.N., Kalikhman A.D., Radionov V.V. About dynamics of traveling ionospheric disturbances. *Issledovaniya po geomagnetizmu, aeronomii i fizike Solntsa* [Geomagnetism, Aeronomy and Solar Physics Research]. Moscow, Nauka Publ., 1993, vol. 100, pp. 189–196. (In Russian).